ARR No. 3E19

NATIONAL ADVISORY COMMITTEE FOR AERONAUTICS

WARTIME REPORT

ORIGINALLY ISSUED
May 1943 as
Advance Restricted Report 3E19

FORMULAS FOR PROPELLERS IN YAW AND CHARTS OF THE SIDE-FORCE DERIVATIVE

By Herbert S. Ribner

Langley Memorial Aeronautical Laboratory
Langley Field, Va.

NACA

WASHINGTON

NATIONAL ADVISORY COMMITTEE FOR AERONAUTICS

ADVANCE RESTRICTED REPORT

FORMULAS FOR PROPELLERS IN YAW AND CHARTS OF THE SIDE-FORCE DERIVATIVE

By Herbert S. Ribner

SUMMARY

General formulas are given for propellers for the rate of change of side-force coefficient with angle of yaw and for the rate of change of pitching-moment coefficient with angle of yaw. Charts of the side-force derivative are given for two propellers of different plan form. The charts cover solidities of two to six blades and single and dual rotation. The blade angles range from 15° or 20° to 60°.

The equations, and the charts computed from the equations, are based on an unpublished analysis, which incorporates factors not adequately covered in previously published work and gives good agreement with experiment over a wide range of operating conditions. A study of the equations indicates that they are consistent with the following physical interpretation: In developing side force, the propeller acts like a fin of which the area is the projected side area of the propeller, the effective aspect ratio is of the order of 8, and the effective dynamic pressure is roughly that at the propeller disk as augmented by the inflow. The variation of the inflow velocity, for a fixed-pitch propeller, accounts for most of the variation of side force with advance-diameter ratio.

The charts may be applied to obtain the rate of change of normal-force coefficient with angle of attack of the axis of rotation if proper account is taken of the upwash or downwash from the wing.

INTRODUCTION

There has been a need in stability analyses for a systematic series of charts for the estimation of the rate

of change of propeller side force with angle of yaw. Although the formula developed by Harris and Glauert in references 1 and 2 and discussed in reference 3, which expresses the side force in yaw in terms of coefficients for the unyawed propeller, is fairly satisfactory, there has been no adequate formula based primarily on the geometry of the propeller blades. An unpublished analysis has resulted in such a formula. The basic assumptions are similar to those of the vortex theory for the uninclined propeller when the Goldstein correction for finite number of blades is omitted. Comparison with a number of experimental results has indicated that the accuracy of ±10 percent obtainable by the analytical method is of the order obtained by the uncorrected vortex theory for the uninclined propeller.

The formula, developed in the analysis and given herein, has been used to prepare a series of charts giving the rate of change of side-force coefficient with angle of yaw as a function of the advance-diameter ratio V/nD; the blade angle and solidity are parameters; the charts cover both single and dual rotation. The computations were made for two representative propellers, the Hamilton Standard 2155-6 and the NACA 10-3062-045. Means are given for interpolating for other propellers.

In order to make the present report complete in itself and to make the charts more intelligible, formulas for the side-force and pitching-moment derivatives are given at the outset with an explanatory text. The other propeller stability derivatives with respect to yaw are zero.

For the purpose of expediting the publication of the charts, the derivation of the formulas has been omitted from the present paper. There is included herein, however, a graph that shows a comparison of the theoretical values with the experimental data of Lesley, Worley, and Hoy (reference 4).

SYMBOLS

The formulas of the present report refer to a system of body axes. For single-rotating propellers, the origin is at the intersection of the axis of rotation and the

plane of rotation; for dual-rotating propellers, the origin is on the axis of rotation halfway between the planes of rotation of the front and rear propellers. The X axis is coincident with the axis of rotation and is directed forward; the Y axis is directed to the right; and the Z axis is directed downward. The symbols are defined as follows:

D	propeller diameter
R	tip radius
r	radius to any blade element
S'	disk area $(\pi D^2/4)$
x	fraction of tip radius (r/R)
x_o	minimum fraction of tip radius at which shank blade sections develop lift (taken as 0.2)
x_s	ratio of spinner radius to tip radius
B	number of blades
b	blade section chord
σ	solidity at 0.75R $\left[\frac{4B}{3\pi}\left(\frac{b}{D}\right)_{0.75R}\right]$
β_o	blade angle to zero-lift chord
β	blade angle to reference chord, measured at 0.75R station, degress
p	geometric pitch
ψ	angle of yaw, radians
α_T	angle of attack of thrust axis, radians
V	free-stream velocity
q	free-stream dynamic pressure $(1/2\,\rho V^2)$
a	inflow factor

V_a axial velocity at propeller disk $[V(1 + a)]$

$f(a)$ q-factor $\left[(1 + a)\dfrac{(1 + a) + (1 + 2a)^2}{1 + (1 + 2a)^2}\right]$

C_T thrust coefficient $(\text{thrust}/\rho n^2 D^4)$

T_c thrust coefficient $(\text{thrust}/\rho V^2 D^2$ or $C_T/J^2)$

n rotational speed, revolutions per second

J advance-diameter ratio (V/nD)

ϕ effective helix angle

$\left\{\tan^{-1}[V_a/(2\pi nr - \text{slipstream rotational velocity})]\right\}$

Y side force (body axes)

Z normal force

M pitching moment (body axes)

$C_{Y'_\psi}$ side-force derivative: rate of change of side-force coefficient with angle of yaw $[(\partial Y/\partial\psi)/qS']$

$C_{M'_\psi}$ pitching-moment derivative: rate of change of pitching-moment coefficient with angle of yaw $[(\partial M/\partial\psi)/qDS']$

m_o average slope of section lift curve per radian (taken as $0.95 \times 2\pi$)

k_s spinner factor

k_a sidewash factor

K constant in the equation for k_s

I_1 side-area index

Δ defined by equation (2a) (zero for dual-rotating propellers)

I_2 integral defined by equation (2b)

I_3 integral defined by equation (2c)

m defined by equation (3a)

Subscripts:

$0.75R$ measured at the 0.75R station ($x = 0.75$)

FORMULAS

Rate of Change of Side-Force Coefficient with Angle of Yaw for Dual-Rotating Propeller

The nature of the formulas for the side-force derivatives makes it simpler to present the formula for the dual-rotating propeller first. For a dual-rotating propeller, the side-force derivative is

$$C_{Y'_\psi} = \frac{\partial Y/\partial \psi}{qS'} = \frac{k_s f(a)\sigma I_1}{1 + k_a \sigma I_1} \qquad (1)$$

where

the spinner factor $k_s \approx 1.14$

the sidewash factor $k_a \approx 0.4$

the inflow factor $a = (\sqrt{1 + 8T_c/\pi} - 1)/2$

the q-factor $f(a) = \dfrac{(1 + a)[(1 + a) + (1 + 2a)^2]}{1 + (1 + 2a)^2}$ (1a)

the solidity at 0.75R $\sigma = \dfrac{4B}{5\pi}\left(\dfrac{b}{D}\right)_{0.75R}$

the side-area index $I_1 = 3/4\ m_o \displaystyle\int_{x_o}^{1} (b/b_{0.75R}) \sin \beta_o \, dx$

and I_1, $f(a)$, k_s, and k_a are discussed in detail later.

Side-area index I_1.- The product σI_1 is proportional to the area projected by the blades on a plane through the propeller axis. This area may be called the projected side area of the propeller. The significant factor I_1 has been termed "the side-area index"; σ is the solidity at the 0.75R station. In equation (1), $k_a\sigma I_1$ is always small in comparison with unity, with the result that C_Y/ψ is approximately proportional to σI_1 and hence to the projected side area of the propeller. The factor $1/(1 + k_a\sigma I_1)$ may be regarded as a correction for aspect ratio.

If graphical integration is inconvenient, the side-area index I_1 may be evaluated quite simply and with sufficient accuracy by Gauss' rule for approximate integration (reference 5), which ordinarily requires fewer ordinates than Simpson's rule for the same accuracy. Details are given in the appendix.

The q-factor f(a).- By the definition of a, the expression $V(1 + a)$ is the axial wind velocity at the propeller disk. Accordingly, $(1 + a)^2q$ is the dynamic pressure at the propeller disk. The value of $f(a)q$ is only slightly less than $(1 + a)^2q$ for moderate inflows. Equation (1) shows, therefore, that the side force for a given angle of yaw is roughly proportional to the dynamic pressure at the propeller disk as augmented by the inflow. A chart of the variation of $f(a)$ with T_C is given in figure 1.

Spinner factor k_s.- If the propeller is provided with a spinner in combination with a liquid-cooled nacelle, the circumferential component of the side wind due to yaw is considerably increased in the region of the blade shanks. This circumstance increases the side force by a factor k_s which is closely given by

$$k_s = 1 + \frac{K \int_{x_0}^{1} (r_s/x)^2 (b/b_{0.75R}) \sin \beta_0 \, dx}{\int_{x_0}^{1} (b/b_{0.75R}) \sin \beta_0 \, dx} \qquad (1b)$$

where x_s is the ratio of the spinner radius to the tip radius and K is a constant which is approximately 0.90 for a nacelle fineness ratio of 6 and 1.00 for a fineness ratio of infinity. For the spinners of present-day usage, k_s is of the order of 1.14 ± 0.04.

A similar effect undoubtedly occurs when spinners are used with air-cooled nacelles, but the estimation of k_s is more difficult. It is recommended that the factor 1.14 be used.

Sidewash factor k_a.- The reduction of side force due to the sidewash of the slipstream is accounted for by the sidewash factor k_a and by the deviation of $f(a)$ from the value $(1 + a)^2$. The accurate expression for k_a is

$$k_a = \frac{(1 + 2a)^2}{4[1 + (1 + 2a)^2]} \frac{\int_{x_o}^{1} (b/b_{0.75R})^2 \sin^2 \beta_o \, dx/x}{\left[\int_{x_o}^{1} (b/b_{0.75R}) \sin \beta_o \, dx\right]^2} \qquad (1c)$$

The effect is analogous to the reduction of wing lift by downwash. An average value of k_a is 0.4.

Required accuracy, k_s and k_a.- To the degree in which comparison with existing experiments establishes the accuracy - about ±10 percent - of the side-force formulas, it is sufficiently accurate to use the mean value 0.4 for k_a and, for the usual size spinner ($x_s = 0.16$), 1.14 for k_s.

Physical interpretation of propeller in yaw.- A study of equations (1) and (2) in light of the discussion of the side-area index I_1 and the q-factor $f(a)$, with data for representative propellers, shows that the equations are consistent with the following physical interpretation: In developing side force in yaw, the propeller acts like a fin of which the area is the projected side area of the propeller. (The projected side area is the area projected by the blades on a plane through the axis of rotation. For two or one blade, this area varies with azimuth; but the text refers to the average value, which

is given to a close approximation by one-half the number of blades times the area projected by a single blade on a plane containing the blade center line and the axis of rotation.) This equivalent fin may with small error be regarded as situated in the inflow at the propeller disk and subject to the corresponding augmented dynamic pressure. The variation of inflow velocity therefore acccunts for most of the variation of side force with advance-diameter ratio, for a fixed-pitch propeller.

The effective aspect ratio of the projected side area is of the order of two-thirds the geometric aspect ratio with dual rotation. The effective aspect ratio is much less with single than with dual rotation; the smaller aspect ratio accounts for a reduction in the side force, which for the six-blade Hamilton Standard propeller 3155-6 varies from 4 percent at $\beta = 55^\circ$ to 24 percent at $\beta = 15^\circ$. A mean value of the effective aspect ratio for single- and dual-rotating propellers of present-day usage is 8.

Rate of Change of Side-Force Coefficient with Angle of Yaw for Single-Rotating Propeller

For a single-rotating propeller, the side-force derivative is

$$C_{Y'_\psi} = \frac{\partial Y/\partial\psi}{qS'} = \frac{k_s f(a)\sigma I_1}{I_1/(I_1 - \Delta) + k_a \sigma I_1} \tag{2}$$

The definitions of equation (1) still apply and

$$\Delta = \frac{\left(\sigma I_2 - J\,\frac{2a}{\pi}\right)\left(\sigma I_2 + 2J\,\frac{2a}{\pi}\right)}{\sigma(1 + \sigma I_3)} \tag{2a}$$

where

$$I_2 = \frac{3}{4}\, m_o \int_{x_o}^{1} (b/b_{0.75R} \cos\beta_o\, x\,dx \tag{2b}$$

$$I_3 = \frac{3}{4}\, m_o \int_{x_o}^{1} \frac{b}{b_{0.75R}}\,\frac{\cos^2\phi}{\sin\phi}\, x^2 dx \tag{2c}$$

A family of approximate curves of I_2 are given in figure 2 as functions of V/nD, with the solidity σ as the parameter. The curves are applicable for blade-angle settings at a given value of V/nD in the range in which the blades are not stalled. The data of figure 2 were computed for a definite propeller, Hamilton Standard 3155-6, but may be applied to any other propeller with negligible error in $C_{Y'_\psi}$. The variation of $2a/\pi$ with T_c is given in figure 3.

The term Δ is positive over the operating range of the propeller in flight and is roughly one-tenth of I_1. Comparison of equation (2) for single rotation with equation (1) for dual rotation shows that the effect of positive Δ is a reduction in $C_{Y'_\psi}$ — that is, a single-rotating propeller experiences less side force in yaw than the corresponding dual-rotating propeller.

The reduction in side force in yaw reaches 24 percent for low blade angles: its average is 15 percent. The reduction is explained by the fact that the asymmetry of disk loading, which for the single-rotating propeller produces the pitching moment due to yaw, also induces a component of flow tending to reduce the effect of the angle of yaw. For dual-rotating propellers, there is no resultant asymmetry because the asymmetries of the disk loadings of the two sections are so disposed as to compensate.

Rate of Change of Pitching Moment with Angle of Yaw

For a dual-rotating propeller, the pitching-moment derivative is approximately zero for the reason previously mentioned. For a single-rotating propeller, this derivative is given by

$$C_{M'_\psi} = \frac{\partial M/\partial \Psi}{qDS'} = \pm \frac{k_s f(a) m}{1 + k_a \sigma (I_1 - \Delta)} \qquad (3)$$

where the positive sign is to be taken for a right-hand propeller and the negative sign, for a left-hand propeller.

The definitions previously given are applicable here and

$$m = \frac{\sigma I_2 + 2J \frac{2a}{\pi}}{2(1 + \sigma I_3)} \tag{3a}$$

SIDE-FORCE CHARTS

Formulas (1) and (2) have been used to compute a series of charts of the side-force derivative

$$C_{Y,\psi} = \frac{\partial Y / \partial \psi}{\rho S}$$

This derivative, otherwise interpreted, is approximately twice the area of an equivalent fin of average aspect ratio divided by the disk area.

Each chart gives the variation of $C_{Y,\psi}$ with V/nD for a range of blade angles and applies to a definite solidity. There is a series of charts for each of two blade forms. One blade form is a conventional type, Hamilton Standard 3155-6, with a plan form almost symmetrical about the maximum chord, which is at approximately the 0.6CR station. The other blade form, NACA 10-3062-045, has a wide, almost uniform chord out to the 0.75R station and a rounded tip section. The plan forms and pitch distributions for the two propellers are shown in figure 4.

Hamilton Standard propeller 3155-6.- The charts of figures 5 to 9 apply to Hamilton Standard propeller 3155-6. Figures 5, 6, 7, and 8 are for the two-, three-, four-, and six-blade single-rotating propellers, respectively. Figure 9 is for a six-blade dual-rotating propeller. The solidity σ varies from 0.061 for the two-blade propeller to 0.182 for the six-blade propellers.

A liquid-cooled nacelle of fineness ratio 6 was assumed and the spinner diameter was taken as 0.164 times the propeller diameter in determining the spinner factor k_s. The average value of k_s, which depends slightly on the blade-angle setting, is about 1.125. This value signifies that, on the average, 12.5 percent has been added to the values which would be obtained in the absence of a spinner.

The values of T_c used in the computations were obtained from figures 24 and 26 of reference 6 for the 25° and 45° blade angles and were interpolated for the other blade angles with the aid of figure 15 of reference 7.

NACA propeller 10-3062-045.- The charts of figures 10 to 13 apply to NACA propeller 10-3062-045. Figures 10, 11, and 12 are for the two-, three-, and four-blade single-rotating propellers, respectively. Figure 13 is for a six-blade dual-rotating propeller. The solidity σ varies from 0.0825 for the two-blade propeller to 0.247 for the six-blade propeller.

The spinner-nacelle proportions were taken the same as for Hamilton Standard propeller 3155-6, and the corresponding average value of the spinner factor k_s is 1.15.

The values of T_c used in the computations were obtained from unpublished experimental curves for the three-blade single-rotating propeller. The curves were extrapolated for fewer blades and for more blades and for dual rotation with the aid of figures 24 and 26 of reference 6. It is believed that the errors in $C_{Y'_\psi}$ introduced by errors in the extrapolation are within 2 or 3 percent.

Comparison with experiment.- Figure 14 presents the variation of the side-force derivative with advance-diameter ratio for the two-blade model propeller of reference 4. Curves computed from the formulas of the present report are plotted with the experimental values.

Interpolation for blade shape and solidity.- The computations show that, within the usual range, blade twist has a relatively small effect on $C_{Y'_\psi}$. The three important parameters are solidity, blade angle at 0.75R, and plan form, for a given V/nD. The charts for a given plan form may be interpolated linearly from the charted values for variations of solidity σ and blade angle β.

The determination of $C_{Y'_\psi}$ for plan forms between those of Hamilton Standard propeller 3155-6 and NACA propeller 10-3062-045 would be expected to require a double interpolation, one for solidity, because the two

propellers are not charted at the same solidities, and a second one for plan form. A simpler procedure results from the following considerations:

For a given solidity, it is found that the plan form of the NACA propeller 10-3068-045 yields about 13 percent more side force than does the plan form of the Hamilton Standard propeller 3155-6 at the same V/nD. The factor 1.13 holds within 2 or 3 percent near the line of zero thrust although the error increases to about 6 percent at low V/nD and high thrust. To this accuracy the side-force coefficient for a propeller of a given plan form and solidity $\sigma = 0.091$, for example, could be estimated from the $\sigma = 0.091$ chart of Hamilton Standard propeller 3155-6 by comparing the given plan form with the plan forms of Hamilton Standard 3155-6 and NACA 10-3068-045 propellers in figure 4 and increasing the ordinates from the chart by the appropriate fraction of 13 percent. In making the plan-form comparison, most weight should be given the root sections of the blade. If the solidity σ does not correspond to that of one of the charts, two charts of different solidity for the same propeller may be interpolated linearly.

Use of charts for propellers in pitch.- The charts with pitch substituted for yaw can be used to obtain the rate of change of normal force with angle of attack of thrust axis, if the influence of the wing on the angle of flow at the propeller is included. The upwash can be taken into account, if the propeller is in front of the wing, by multiplying the value of $C_{Y'_\psi}$ - now interpreted as $-C_{y'_{\alpha_T}} = -\frac{\partial Z/\partial \alpha_T}{qS'}$ - by 1 plus the rate of change with angle of attack of the angle of upwash induced at the propeller by the wing. If the propeller is behind the wing, the factor should be 1 minus the rate of change with angle of attack of the angle of downwash induced at the propeller by the wing.

CONCLUDING REMARKS

Equations for propellers in yaw and charts of the side-force derivative have been given herein for single- and dual-rotating propellers in terms of a side-area index and a dynamic-pressure factor, which is a function of the

inflow factor. The study of these equations indicates that they are consistent with the following physical interpretation: In developing side force, the propeller acts like a fin of which the area is the projected side area of the propeller, the effective aspect ratio is of the order of 8, and the effective dynamic pressure is roughly that at the propeller disk as augmented by the inflow. The variation of the inflow velocity, for a fixed-pitch propeller, accounts for most of the variation of side force with advance-diameter ratio.

Langley Memorial Aeronautical Laboratory,
National Advisory Committee for Aeronautics,
Langley Field, Va.

APPENDIX

Gauss' rule for approximate integration may be expressed by the relation

$$\int_{x_0}^{x_{n+1}} f(x)dx \approx P_1 f(x_1) + P_2 f(x_2) + \ldots + P_n f(x_n)$$

where x_1 to x_n are certain abscissas and P_1 to P_n are Gauss' coefficients. For the integrals of the present report, five ordinates are found to be sufficient to determine C_{l_ψ} within 1 percent. For x_0 taken as 0.2 and x_{n+1} taken as 1, the appropriate values are

$x_1 = 0.258$	$P_1 = 0.095$
$x_2 = 0.385$	$P_2 = 0.191$
$x_3 = 0.600$	$P_3 = 0.228$
$x_4 = 0.815$	$P_4 = 0.191$
$x_5 = 0.963$	$P_5 = 0.095$

As an example, the integral $\int_{x_0}^{1} (b/b_{0.75R}) \sin \beta_0 \, dx$ which occurs in I_1 may be evaluated as

$$0.036 \frac{(b/D)_{0.238R}}{(b/D)_{0.75R}} \sin \beta_{0\,0.238R} + 0.191 \frac{(b/D)_{0.385R}}{(b/D)_{0.75R}} \sin \beta_{0\,0.385R}$$

$$+ 0.326 \frac{(b/D)_{0.600R}}{(b/D)_{0.75R}} \sin \beta_{0\,0.600R} + 0.191 \frac{(b/D)_{0.815R}}{(b/D)_{0.75R}} \sin \beta_{0\,0.815R}$$

$$+ 0.036 \frac{(b/D)_{0.963R}}{(b/D)_{0.75R}} \sin \beta_{0\,0.963R}$$

where $\frac{b/D}{(b/D)_{0.75R}}$ has been written for its equivalent $b/b_{0.75R}$ in recognition of the practice of using b/D as the plan-form variable.

REFERENCES

1. Harris, R. G.: Forces on a Propeller Due to Sideslip. R. & M. No. 427, British A.C.A., 1918.

2. Glauert, H.: The Stability Derivatives of an Airscrew. R. & M. No. 642, British A.C.A., 1919.

3. Goett, Harry J., and Pass, H. R.: Effect of Propeller Operation on the Pitching Moments of Single-Engine Monoplanes. NACA A.C.R., May 1941.

4. Lesley, E. P., Worley, George F., and Hoy, Stanley: Air Propellers in Yaw. Rep. No. 597, NACA, 1937.

5. Munk, Max M.: Fundamentals of Fluid Dynamics for Aircraft Designers. The Ronald Press Co., 1929, p. 79.

6. Runckel, Jack F.: The Effect of Pitch on Force and Moment Characteristics of Full-Scale Propellers of Five Solidities. NACA A.R.R., June 1942.

7. Diermann, David, and Hartman, Edwin P.: Tests of Two Full-Scale Propellers with Different Pitch Distributions, at Blade Angles up to 60°. Rep. No. 658, NACA, 1939.

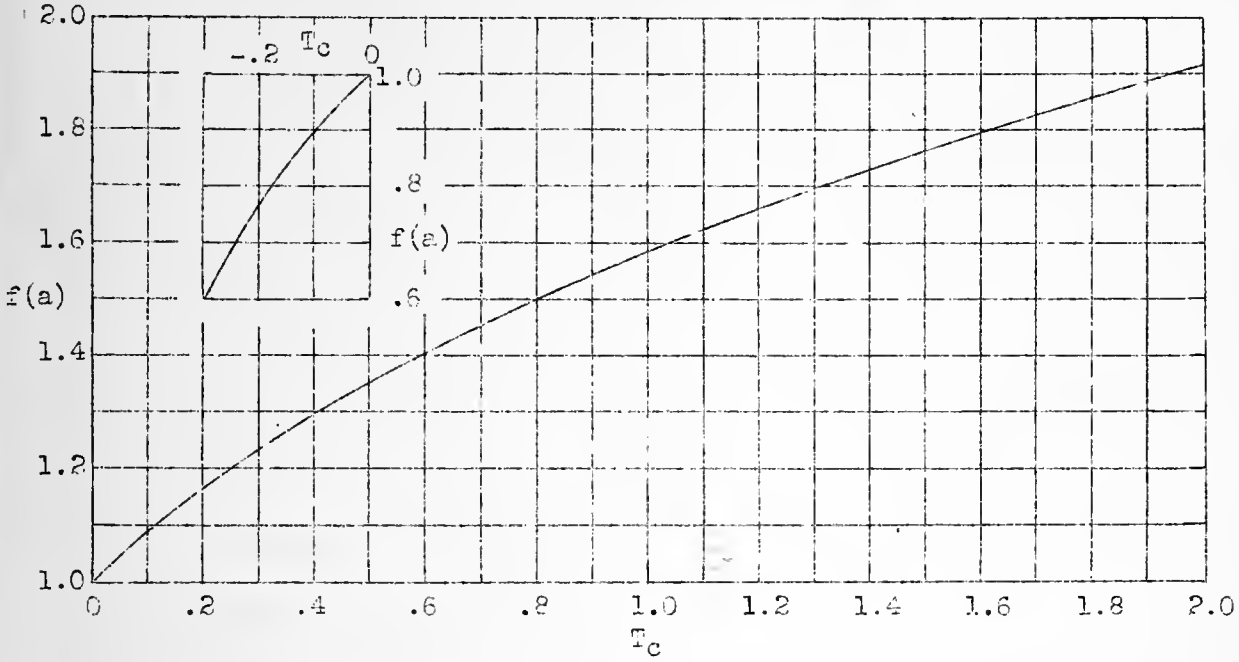

Figure 1.- Variation of a-factor f(a) with T_c. $T_c = C_T/(V/nD)^2$.

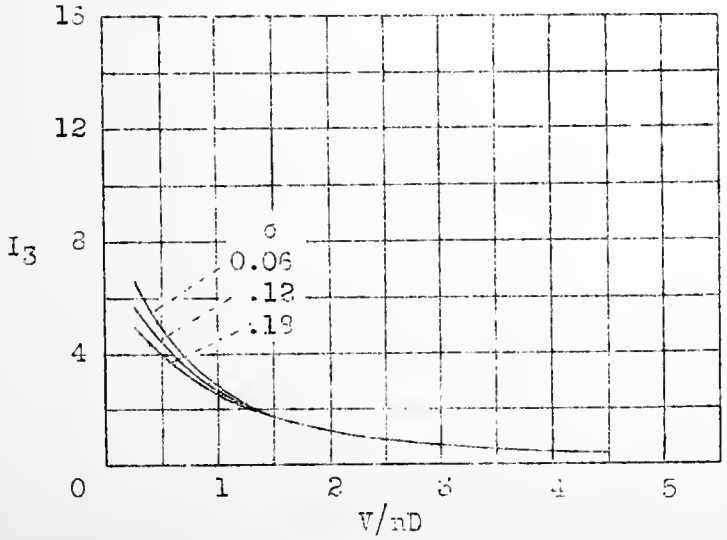

Figure 2.- Variation of I_3 with V/nD and solidity. Approximate curves for blade-angle settings at which the blades

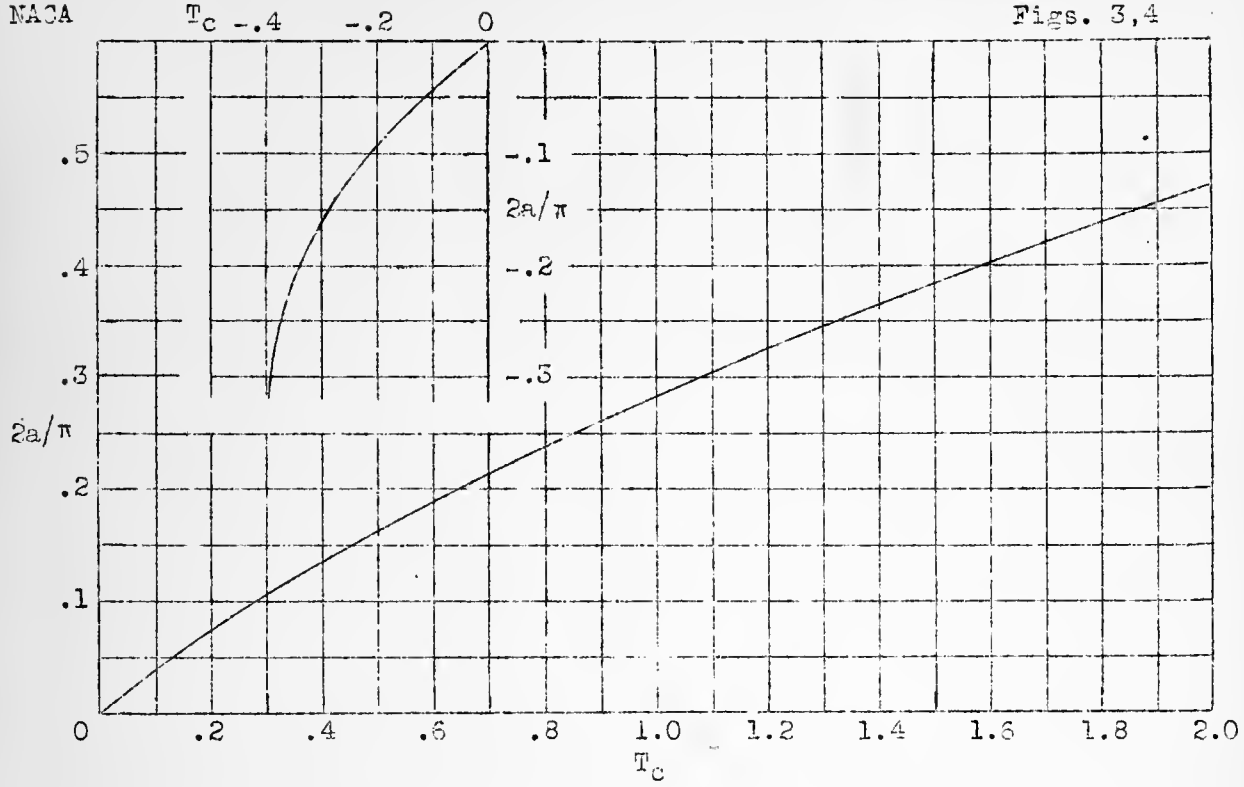

Figure 3.- Variation of $2a/\pi$ with T_c. $T_c = C_T/(V/nD)^2$.

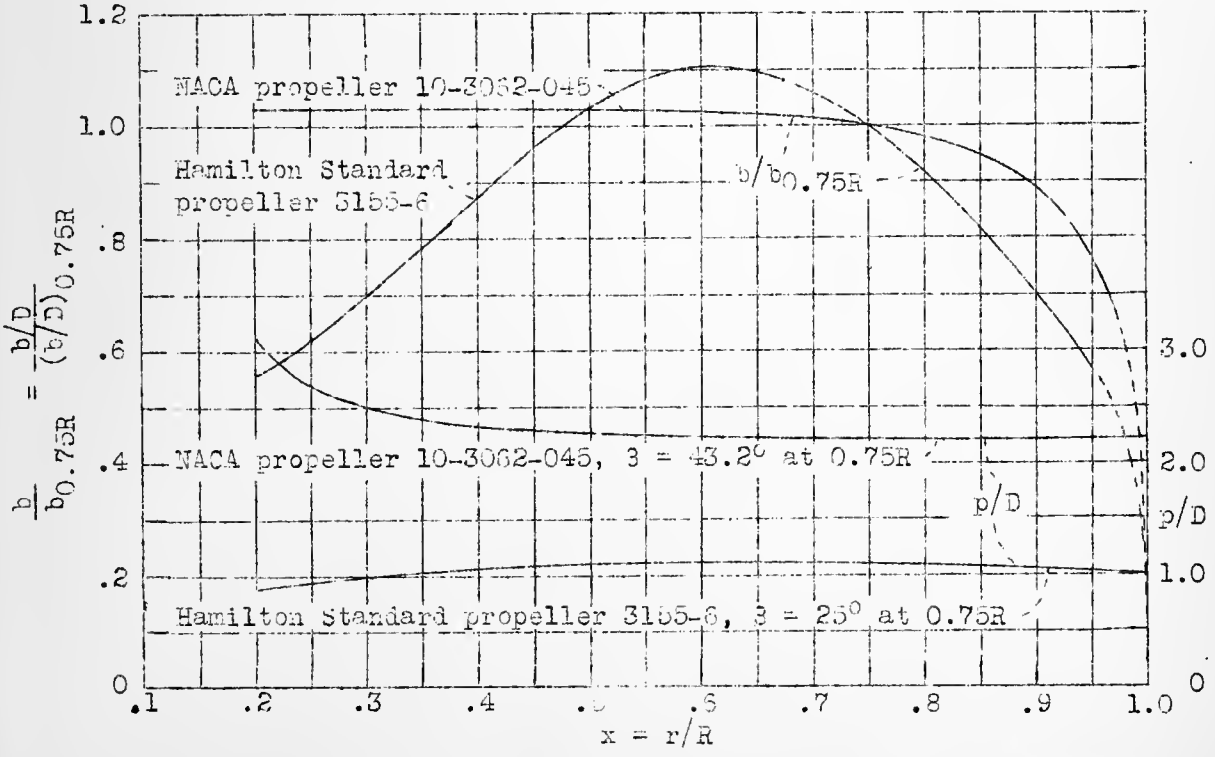

Figure 4.- Plan forms and pitch distributions of NACA 10-3062-045 and Hamilton Standard 3155-6 propellers.

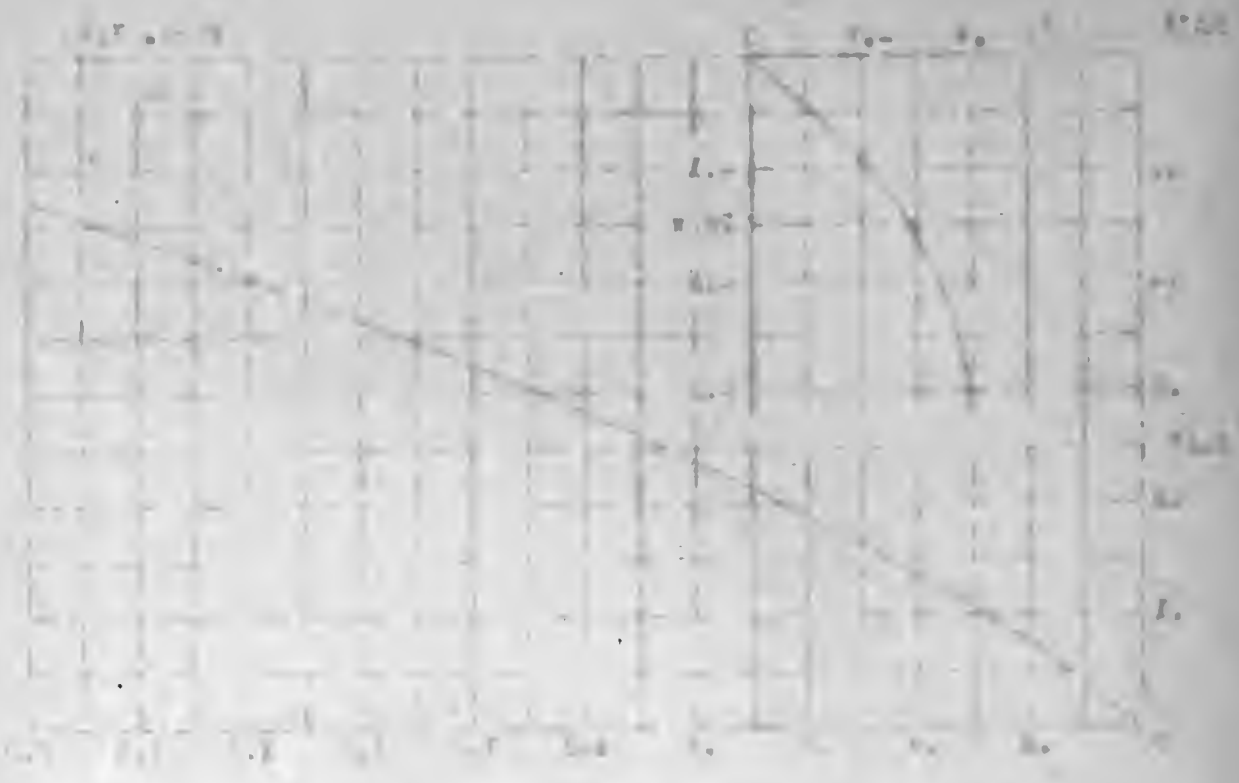

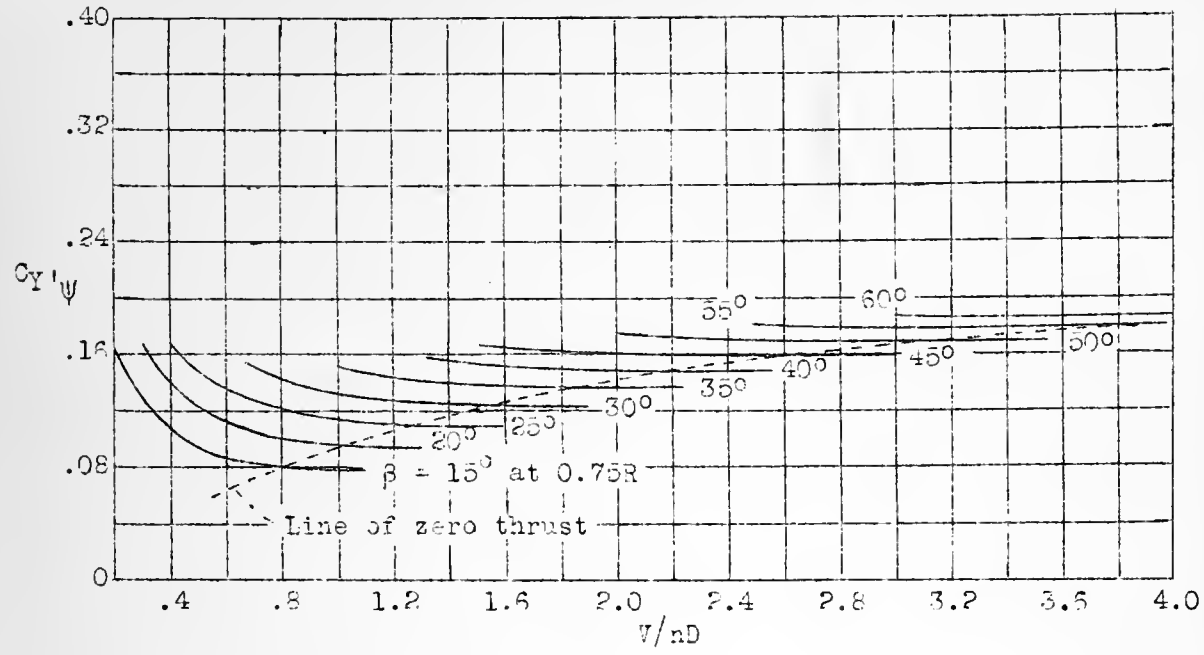

Figure 5.- Side-force derivative for single-rotating Hamilton Standard propeller 3155-6 with spinner. Two blades, σ, 0.061.

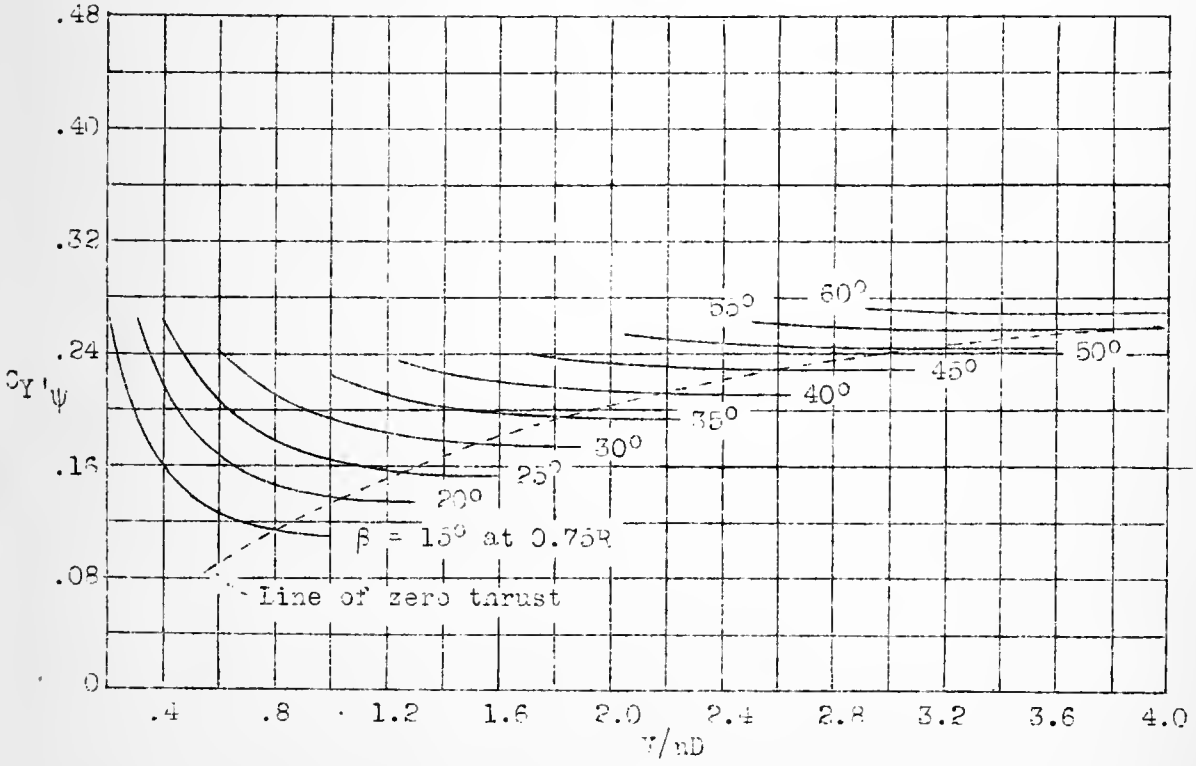

Figure 6.- Side-force derivative for single-rotating Hamilton Standard propeller 3155-6 with spinner. Three blades, σ, 0.091.

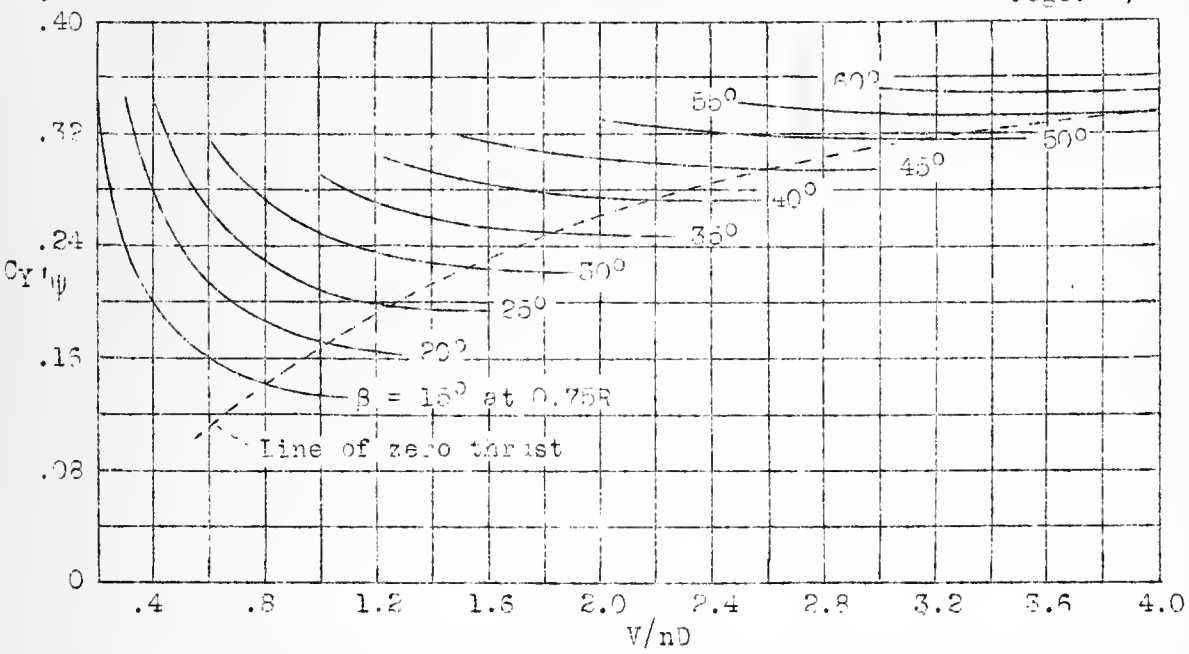

Figure 7.- Side-force derivative for single-rotating Hamilton Standard propeller 3155-6 with spinner. Four blades, σ, 0.121.

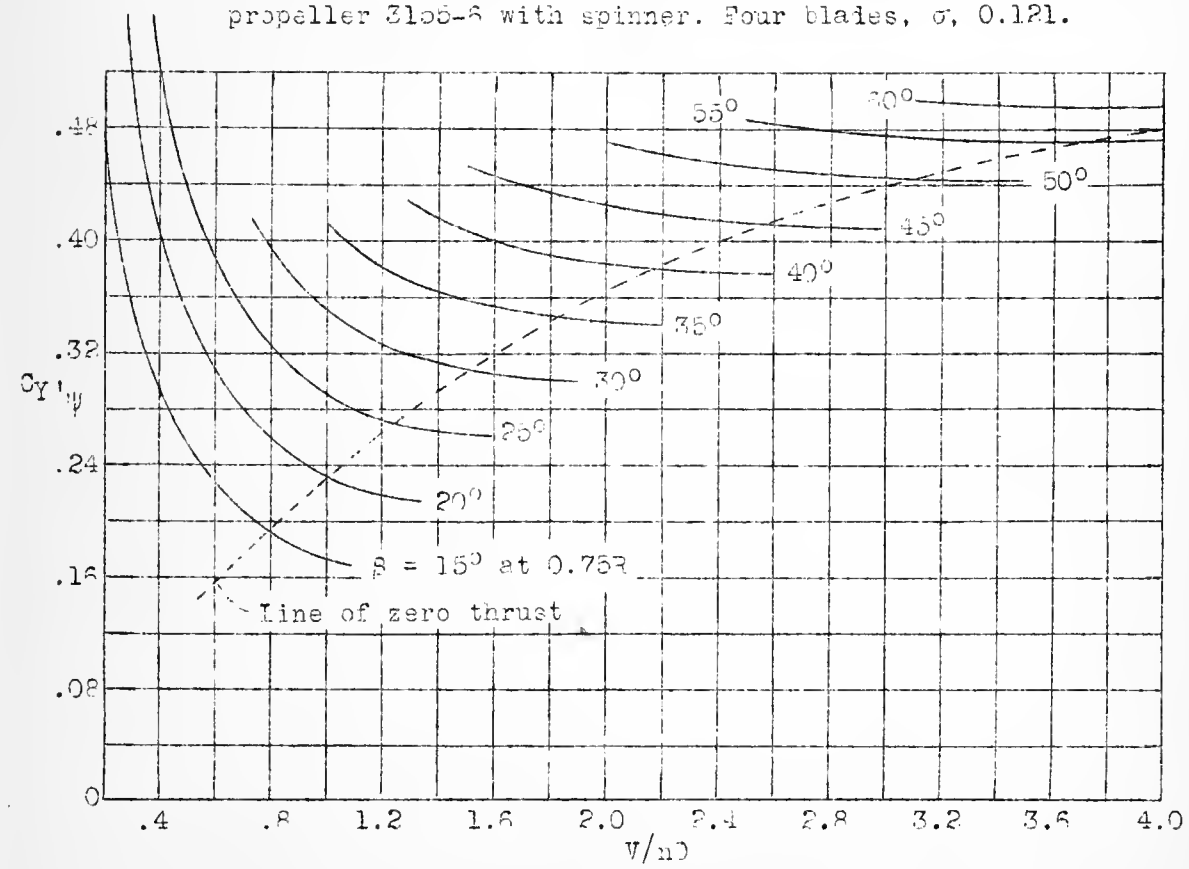

Figure 8.- Side-force derivative for single-rotating Hamilton Standard propeller 3155-6 with spinner. Six blades, σ, 0.182.

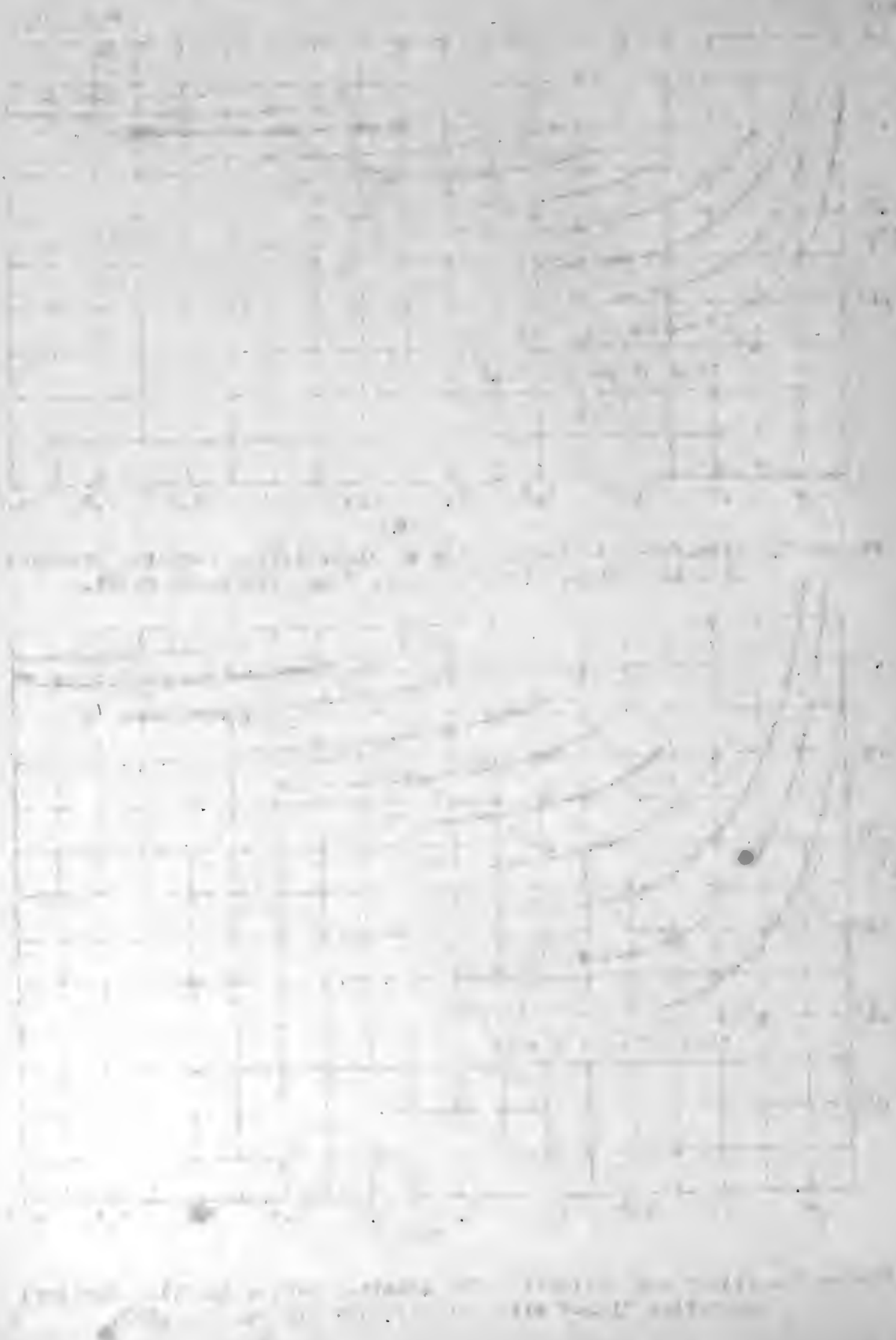

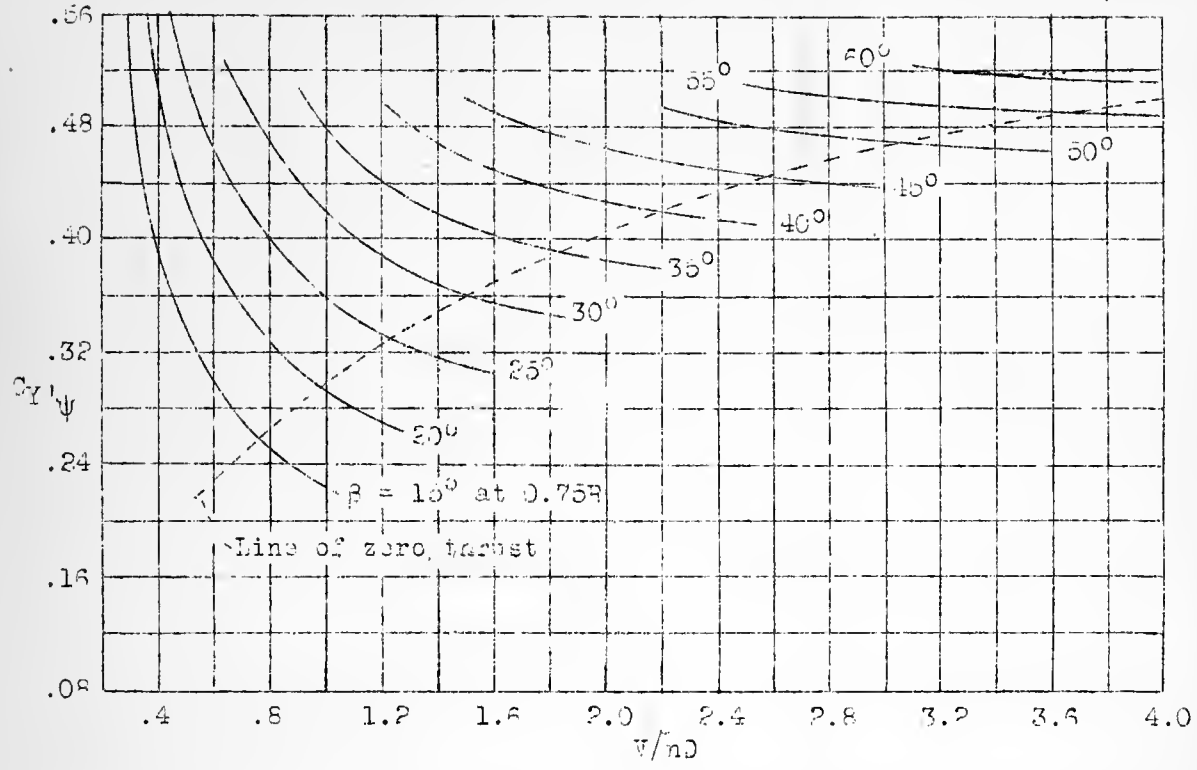

Figure 9.- Side-force derivative for dual-rotating Hamilton Standard propeller 3155-6 with spinner. Six blades, σ, 0.182.

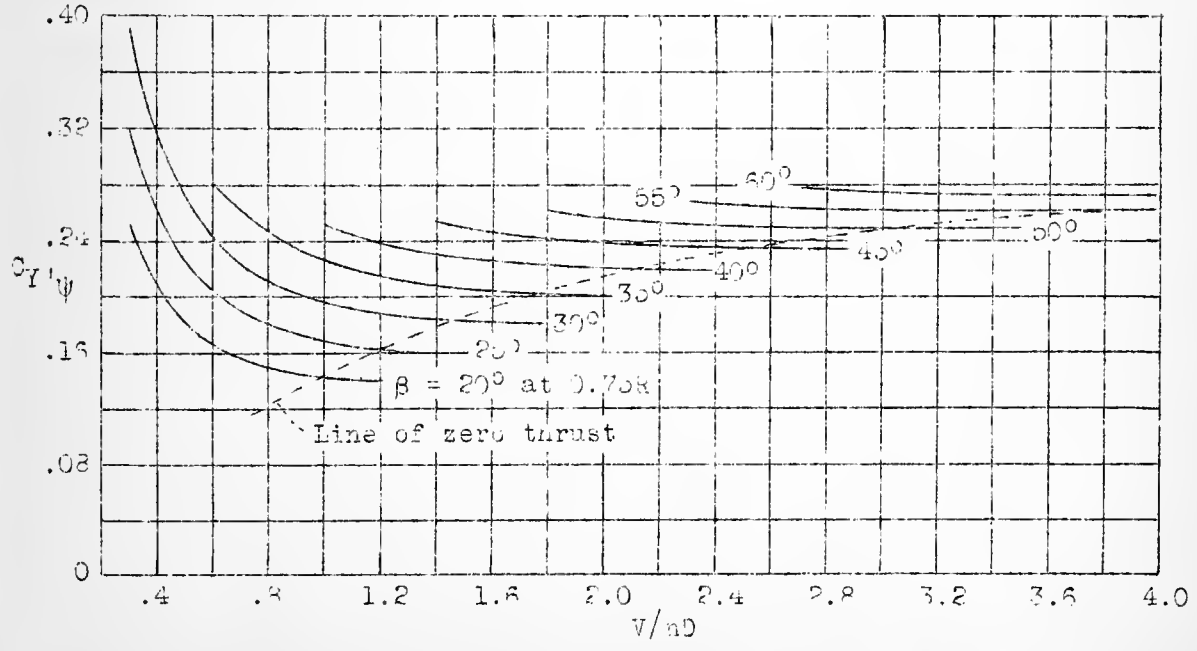

Figure 10.- Side-force derivative for single-rotating NACA propeller 10-3062-045 with spinner. Two blades, σ, 0.0825.

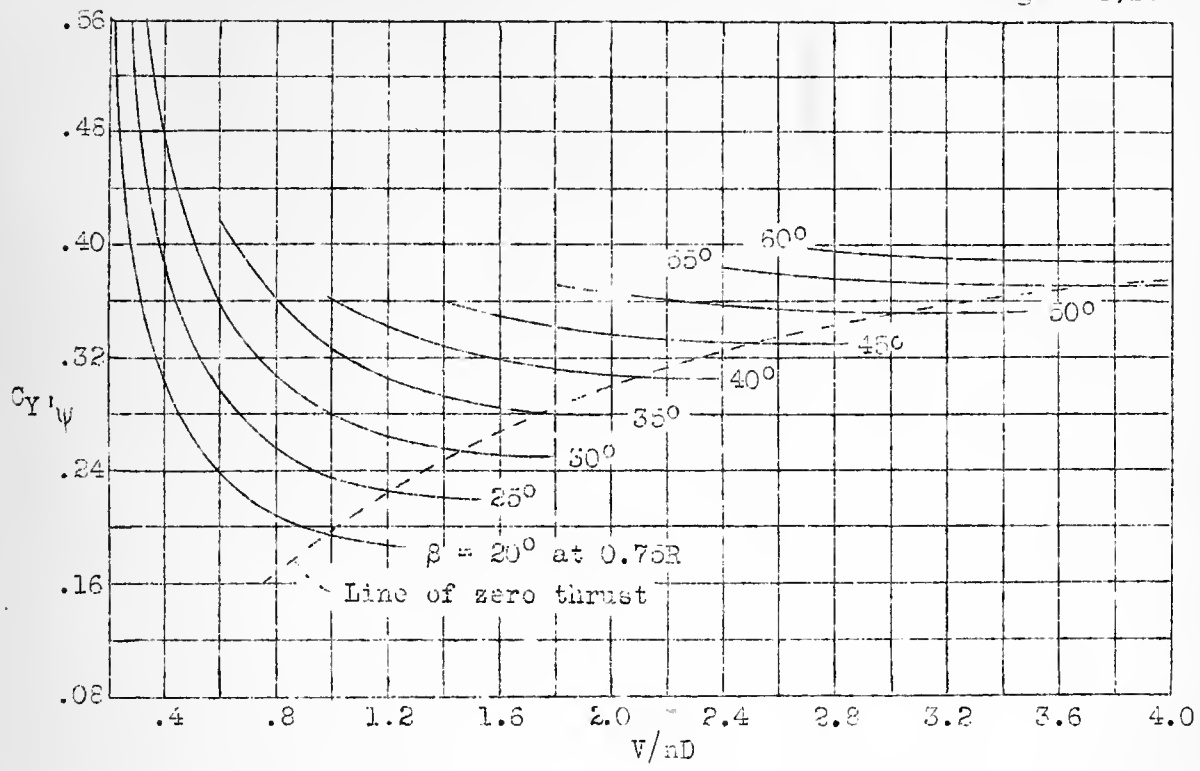

Figure 11.- Side-force derivative for single-rotating NACA propeller 10-3062-045 with spinner. Three blades, σ, 0.124.

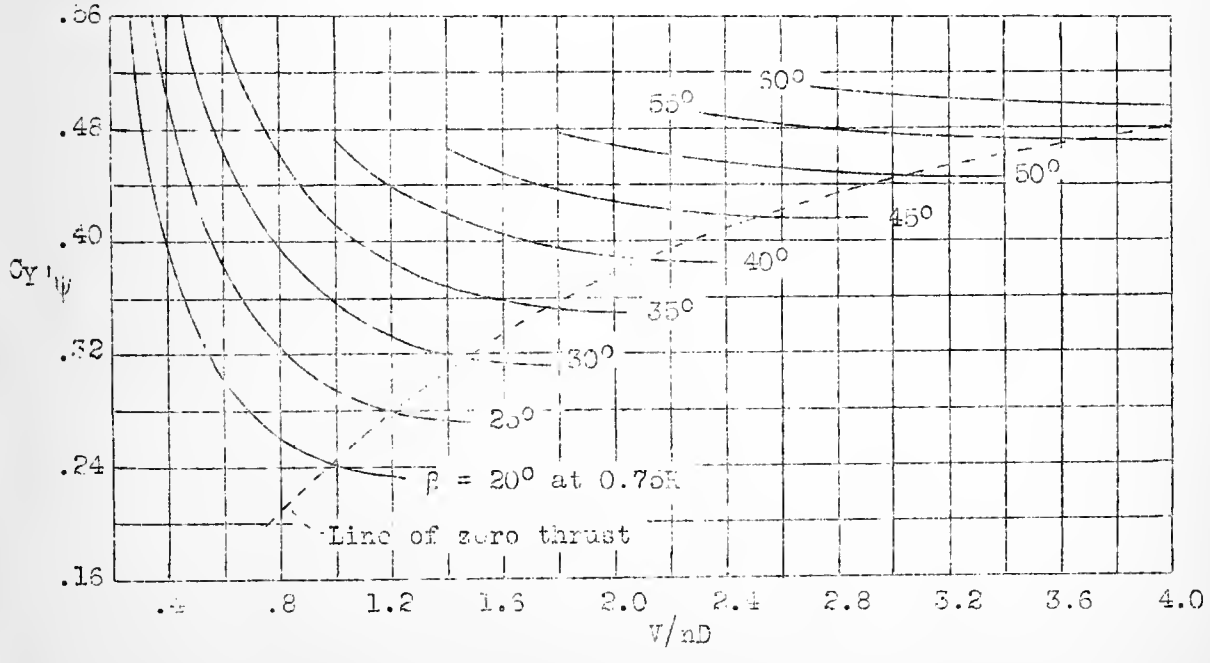

Figure 12.- Side-force derivative for single-rotating NACA propeller 10-3062-045 with spinner. Four blades, σ, 0.165.

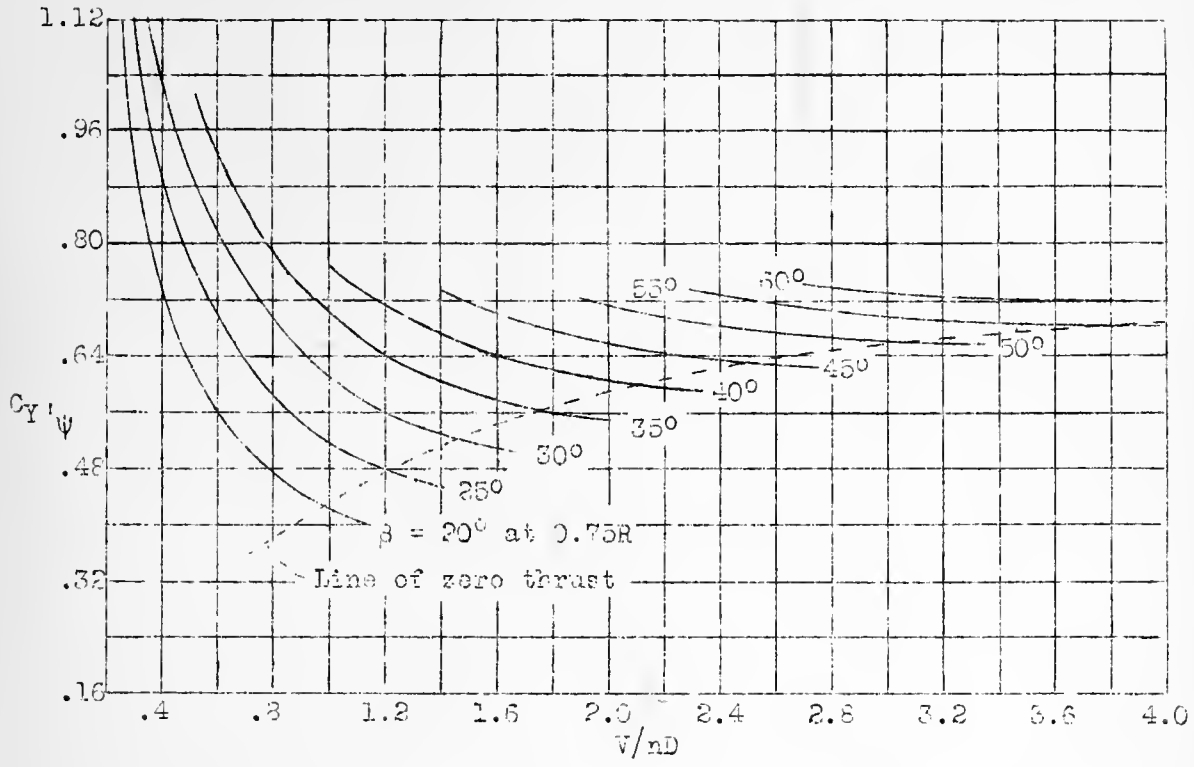

Figure 13.- Side-force derivative for dual-rotating NACA propeller 10-3062-045 with spinner. Six blades, σ, 0.247.

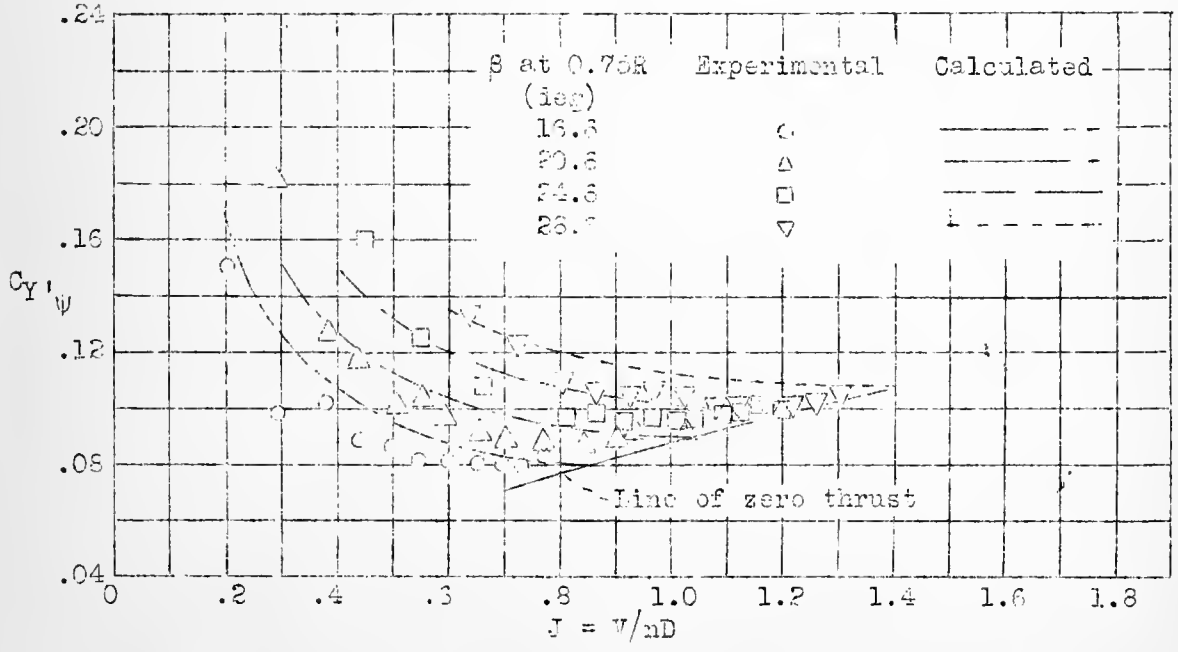

Figure 14.- Comparison of calculated and experimental side-force derivatives for two-blade model propeller. Curves are terminated, except for β = 16.6°, at point where obvious stalling of blades occurs. Experimental data from reference 4.